Bradykinin B_2 receptor-mediated transport into intact cells: anti-receptor antibody-based cargoes

Marie-Thérèse Bawolak[a], Robert Lodge[b], Guillaume Morissette[a], François Marceau[a]

[a]Centre de recherche en rhumatologie et immunologie and [b]Centre de recherche en infectiologie, Centre Hospitalier Universitaire de Québec, Québec QC, Canada G1V 4G2

Corresponding author: Dr F Marceau, Centre Hospitalier Universitaire de Québec, Centre de Recherche en Rhumatologie et Immunologie, CHUQ, Pavillon CHUL, T1-49, 2705 Laurier Blvd., Québec (Québec), Canada G1V 4G2. Tel +1 418 656 4141x46155 ; fax +1 418 654 2767. E-mail address: francois.marceau@crchul.ulaval.ca

Abstract

Endocytosis of the bradykinin-stimulated B_2 receptors is parallel to the transport and subsequent degradation of the ligand. To implement biotechnological applications based on receptor-mediated transport, one strategy is to conjugate the agonist ligand to a cargo. Alternatively, we studied whether the B_2 receptor can transport large antibody-based cargoes into intact cells and characterized the ensuing endosomal routing. Myc-tagged B_2 receptors (coded by the vector myc-B_2R) and a truncated construction devoid of the Ser-Thr phosphorylation domain (myc-B_2R_{trunc} vector) were coupled to anti-myc monoclonal antibodies that did not impair bradykinin binding or elicit calcium signalling in intact cells. Anti-myc antibodies, conjugated or not with secondary antibodies optionally coupled to Qdot nanomaterials, were transported into early endosome autoantigen 1-, and β-arrestin-positive vesicles in bradykinin-stimulated intact cells expressing receptors encoded by myc-B_2R. Antibody-conjugated cargoes progressed into late-endosomes-lysosomes within 3 h without evidence of autophagy. Receptors encoded by myc-B_2R_{trunc} did not support the ligand-controlled endocytosis of anti-myc antibodies. Aside from small ligand-conjugated cargoes, very large antibody-based cargoes can be transported by agonist-stimulated B_2 receptors into intact cells. The latter type of cargo requires a receptor competent for interaction with β-arrestins, enters the degradation pathway separately from the receptor as a function of time and has the potential to confer a qualitatively novel function to a receptor.

Keywords: bradykinin, B_2 receptor, β-arrestin, receptor endocytosis.

1. Introduction

Following agonist stimulation, a specific Ser-Thr-rich C-terminal domain of the bradykinin B_2 receptor is phosphorylated, leading to the recruitment of β-arrestin and adaptor proteins that mediate agonist-induced endocytosis (Leeb-Lundberg et al., 2005). The agonist-stimulated B_2 receptors actually transport and translocate bradykinin into the endosomal compartment, where it is degraded (Munoz and Leeb-Lundberg, 1992). We have recently illustrated B_2 receptor-mediated transport into intact cells using a bradykinin analog conjugated with a carboxyfluorescein cargo (Gera et al., 2011); this agent modelled the endocytic transport, trafficking and intracellular degradation of the peptide ligand.

In the present study, we addressed a novel strategy to exploit receptor-mediated transport for cargoes much heavier than the agonist and showed that receptors encoded by the myc-B_2R vector mediate the endocytosis of anti-myc monoclonal antibodies in HEK 293a cells stimulated with bradykinin, the N-terminal myc epitope merely representing a model for a receptor extracellular epitope that can be recognized by an antibody present in the extracellular space. The routing of both the fluorescent agonist or antibody-based cargoes theoretically hinges on the function of β-arrestins, which was verified using a truncated version of myc-tagged B_2 receptors devoid of the domain substrate for the G protein coupled receptor kinases. Further, the trafficking of receptor-transported cargoes to early endosome autoantigen 1- or Rab7- positive endosomes and lysosomal or autophagic structures was also addressed. This opens the way to exploiting the particular distribution of a given G protein coupled receptor to confer new types of response to cells.

2. Materials and methods

2.1. Drugs and reagents

Cell culture reagents were purchased from Invitrogen. The bradykinin B_2 receptor antagonist LF 16-0687 was a gift from Laboratoires Fournier (Daix, France). Preassembled quantum dot nanocrystals with an average emission wavelength of 705 nm (Qdot 705 goat $F(ab')_2$ anti-mouse IgG conjugate) and BSA-Alexa fluor 594 was purchased from Invitrogen (Carlsbad, CA, USA). All other drugs and reagents were purchased from Sigma-Aldrich (St. Louis, MO, USA).

2.2. Cell culture and transfection

A subclone of HEK 293 cells, called HEK 293a, originally obtained from Sigma-Aldrich was used in all experiments. This cell type was grown in Dulbelcco's modified Eagle's medium supplemented with 10 % FBS, 0.1 % L-glutamine and 0.1 % penicillin-streptomycin. HEK 293a cells were grown until they reached 70 % confluence and were then transfected with one of the myc-B_2R-coding vectors optionally co-transfected with vectors coding for fusion proteins: β-$arrestin_1$-cherry fluorescent protein (CherryFP), β-$arrestin_2$-green fluorescent protein (GFP), or early endosome autoantigen 1 (EEA1)-FYVE-GFP using the EX-Gen 500 transfection reagent (MBI Fermentas Inc., Flameborough, ON, Canada) as recommended by the manufacturer. Vectors coding for the myc-tagged B_2 receptors (myc-B_2R) and its truncated version (myc-B_2R_{trunc} vector) deprived of the substrate domain of the G protein coupled receptor kinase but pharmacologically intact, are described elsewhere (Bawolak et al., 2007; Gera et al., 2011). Briefly, truncation of the C-terminus in the myc-B_2R_{trunc} vector was obtained by mutating Glu^{340} in the myc-B_2R sequence to the stop codon, thus eliminating the 28 C-terminal residues, a

sequence that comprises the conserved and phosphorylable Ser-Thr-rich domain (Leeb-Lundberg et al., 2005). The receptor encoded by myc-B_2R_{trunc} binds [^{3}H]bradykinin with an affinity identical to that of the myc-tagged B_2 receptor, but its surface expression (B_{max}) is slightly inferior to that of the non-truncated construction (Gera et al., 2011). Several plasmids were gifts; the β–arrestin$_2$-GFP fusion protein in pcDNA3 was a kind gift from Dr. M. Bouvier (Université de Montréal, Canada; Bernier et al., 2004). GFP-Rab7 was graciously given by Dr. M. J. Tremblay (Université Laval, Canada) and the vector coding for EEA1-FYVE-GFP, by Dr. Tamas Balla (NICHD, NIH, Bethesda, MD, USA). GFP-LC3 labels autophagosomes in mammalian cells (Kabeya et al., 2000); the pEGFP-LC3 expression vector for this chimerical protein was a generous gift from Dr. T. Yoshimori (Osaka University, Japan).

2.3. Intracellular Ca^{2+} mobilization

To detect the possible agonist effect of anti-myc monoclonal antibodies, Fura-2 fluorometry (Invitrogen) was applied as described (Bawolak et al., 2009).

2.4. Antibody Internalization Assay

The assembly of immune complexes at the cell surface was performed at room temperature and preceded the trafficking experiments at 37°C. Intact HEK 293a cells transiently expressing one of the myc-tagged B_2 receptor constructions (and on occasion, other transgenes) were incubated for 30 minutes at room temperature with anti-myc antibody (clone 4A6, Upstate Biotechnology, Lake Placid, NY; dilution 1:1000). Cells were carefully washed with room-temperature phosphate buffered saline, and further labelled with a goat-anti-mouse IgG-Alexa fluor-594 or -488 coupled antibody (Invitrogen). The incubation time and temperature for both primary and

secondary antibodies were identical. After the cells were washed once with phosphate buffered saline, they were incubated at 37°C in serum-free culture media (1 % penicillin-streptomycin), optionally in the presence of the antagonist LF 16-0687 (1 µM), for 45 minutes preceding a fifteen-minute treatment with the agonist bradykinin (100 nM). Cells were observed at a 1000 × magnification, using green excitation and red emission filters. In additional experiments, cells were transfected with GFP-β-arrestin$_2$, GFP-Rab7 or GFP-LC3, before being subjected to labelling; the same protocol was applied. In some experiments, the incubation time was extended to 3 h at 37°C after bradykinin treatment. Other variants of the anti-myc antibody internalization assay are described in Results (immune complexes visualized using Qdots conjugated with secondary anti-mouse IgG antibodies, dilution 1:50 equivalent to a final concentration of 20 nM; unconjugated anti-myc antibodies detected in fixed and permeabilized cells using a fluorophore-conjugated secondary antibody). Qdots were visualized under ultraviolet excitation using an electronic camera that covered all visible wavelengths.

2.5. Data analysis

The Photoshop software (version 6, Adobe Systems, Mountain View, CA, USA) was used to quantify the endocytosis of fluorescent cargoes into HEK 293a cells from the photographic record (only 1000 ×). For fluorescent immune complexes constructed at the surface of intact cells, the proportion of the plasma membrane-associated ("cortical") fluorescence was determined by subtracting the contribution of the cell image surface corresponding to the cytosol from the total cell fluorescence. The manual delineating of the whole cell surface by the outer white trace and of the cytosolic area by the inner one is illustrated in an example Fig. 1A, the cortical area being the one between the two tracings. The proportion of fluorescence originating

from the cortical area over the total cell fluorescence has been calculated for each evaluated cell. This value was obtained by dividing the fluorescence intensity of the cell surface (number of pixels × average pixel intensity from the "histogram" function) in which the fluorescence of the cytosolic area had been lowered to match the background by the fluorescence of the same whole unretouched cell. The numerical data were averaged for many cells and the effects of cell treatment were statistically evaluated using statistical tests appropriate for the non-normal distributions found: the Mann-Whitney test for pairs of values or the non-parametric Kruskall-Wallis analysis of variance, followed by the Dunn's multiple comparison test to compare pairs of values in experimental designs involving multiple treatments. Proportions of co-localized intracellular vesicles were compared using the χ^2 test. The InStat 3.05 program (GraphPad Software; San Diego, CA) was exploited to compute these tests. Numerical values are reported as means ± S.E.M.

3. Results

The glycoprotein encoded by the myc-B_2R vector is a pharmacologically intact rabbit B_2 receptor construction that has the myc epitope as a N-terminal extracellular extension spatially oriented in such a way that it allows the staining of receptors expressed at the surface of non-permeabilized cells by the monoclonal anti-myc antibody 4A6 (Bawolak et al., 2007). To document the endocytosis of an antibody cargo, intact HEK 293 cells transiently transfected with myc-B_2R were treated with either 4A6 or 9E10 anti-myc monoclonal antibody, washed, further incubated for 45 min, optionally stimulated with bradykinin (10 nM) during the last 15 min of incubation and finally fixed, permeabilized and stained with a secondary fluorescent antibody (Fig. 1). The fluorescence associated to the secondary antibody did not label the cell surface in a manner as continuous as observed with other methods of labelling (e.g., as for the fluorescent antagonist B-10380, Bawolak et al., 2008; Gera et al., 2011), possibly indicating some aggregation ("capping") of immune complexes in live cells. Confocal sections showed that anti-myc antibodies were mostly situated at the cell surface of unstimulated cells, but migrated toward multiple coarse intracellular granules upon bradykinin stimulation. The Photoshop software was used to measure the fluorescence associated with the manually drawn area near to the plasma membrane ("cortical area") versus the intracellular area in replicated experiments (Fig. 2). Although some nonspecific antibody uptake was apparent, this analysis showed the statistically significant endocytosis of both types of anti-myc antibodies following agonist stimulation, the disappearance of the cortical staining being a particularly reliable morphological criterion. An additional control consisted of testing the agonist activity of the anti-myc antibody at the concentration used in all subsequent experiments, clone 4A6, that revealed itself not capable of mobilizing calcium in HEK 293a cells

transiently transfected with myc-B_2R (Fig. 3). In contrast, bradykinin was active in this respect and was not antagonized by the preapplication of the antibody.

A further attempt to test the receptor-mediated endocytosis of even larger cargoes consisted of treating sequentially intact transfected HEK 293a cells (myc-B_2R vector) with the monoclonal 4A6, with a fluorophore conjugated secondary antibody (generally Alexa Fluor 594) or with Qdots conjugated to secondary antibodies and, after re-equilibration in the warmed culture medium, with the agonist. Then the cells, still intact, were observed (data not shown for the fluorescent secondary antibodies; Fig. 4 for imaging of Qdots coated with secondary antibodies; statistical treatment of cortical cell fluorescence in Fig. 5). In Fig. 4, the unremarkable phase contrast appearance of each field is shown solely to identify cells that are illustrated in epifluorescence, the only variable response. Further, as expected from transient receptor transfection, the intensity of fluorescent labeling varies from one cell to another. Within these limitations, the subcellular distribution of the fluorescence associated with the immune complexes was found to be influenced by both the receptor identity and cell treatment with ligands. Surface immune complexes were endocytosed in 15 min in an agonist-dependent manner; further, preincubation with the B_2 receptor antagonist LF 16-0687 (1 μM) prevented much of the endocytosis, as assessed by microscopy (cortical fluorescence). Three h after stimulation with bradykinin, Qdot-associated fluorescence remained intracellular under the form of coarse granules that were generally located deeper relative to the plasma membrane surface (fluorescence intensity may vary; Fig. 4). Nontransfected cells were not labelled by immune complexes constructed at the cell surface (Fig. 4). The receptor construction encoded by myc-B_2R_{trunc} vector, defective for agonist-induced endocytosis (Gera et al., 2011), supported the

construction of Qdot-containing immune complexes at the surface of cells, but these were not translocated into cells upon bradykinin stimulation (Fig. 4, statistical analysis Fig. 5).

Both systems involving immune complex construction at the cell surface followed by agonist-induced endocytosis were further exploited in cells co-transfected with the myc-B_2R vector and that coding for another transgene (Fig. 6). Co-localization statistics have been made on replicated experiments bearing in mind the specific cycling and basal distribution of each marker. GFP-β-$arrestin_2$, which is cytosolic in resting cells but translocates to endosomes in agonist-stimulated cells (Bawolak et al., 2009), was extensively co-localized with the endocytosed immune complexes consisting of antibody-coated Qdots (Fig. 6) upon bradykinin stimulation, indicating that the immune complexes are bound to phosphorylated internalized receptors within 15 min of stimulation. Thus, control cells contained an average of 1.4 ± 0.8 co-localized intracellular particle per cell, whereas 12.9 ± 3.7 were found per agonist-stimulated cell ($P<0.001$, Mann-Whitney test, n = 11 and 17 cells, respectively). Unexpectedly, overexpression of this form of arrestin also resulted in a slightly increased agonist-independent endocytosis of immune complexes in repeated experiments, but those presented no co-localization with GFP-β-$arrestin_2$, and some cell surface labelling was still apparent. Qdot-containing immune complexes were co-localized with the early endosome marker EEA1-FYVE-GFP (Kutateladze et al., 1999; Grosshans et al., 2006) 15 min after bradykinin stimulation (Fig. 6). For this marker, the density of discrete cytosolic particles was similar in both control or bradykinin-stimulated cells (22.3 and 18.6 green particles per cell, respectively), but the proportion of co-localized particules increased sharply upon agonist treatment (10.1% vs. 42.2%, $P<0.001$, χ^2 test, n = 8 and 19 cells, respectively). GFP-Rab7, which labels late endosomes (Marceau et al., 2009), co-localized slightly and progressively with the internalized immune complexes, showing the progression of

the cargo in the endocytic pathway (Fig. 6; photographic record for the 15-min agonist treatment not shown). As observed previously with EEA-1, it was the proportion of Rab7-positive intracellular particules containing the immune complexes, rather than the number of GFP-Rab7 positive vesicles per cell, that varied as a function of agonist treatment and time (control: 4.6% co-localization; bradykinin 15 min: 9.5%, $P<0.01$; bradykinin 3 h: 21.1%, $P<0.0001$ by χ^2 test, n = 18, 16 and 19 cells containing 480, 349 and 389 discrete green particles, respectively). The lack of co-localization with GFP-LC3, a protein associated with the autophagosomes (Kabeya et al., 2000), with immune complex cargoes indicates that, at the 3-hour time point (fig. 6), the Qdot-containing vesicles were not tagged for autophagy (Fig. 6; proportion of co-localized intracellular particles 4.4% in 9 control cells, 6.1% in 19 bradykinin-treated cell, not significantly different by χ^2 test). Alexa Fluor 594-labelled albumin is taken up by cells and ends up in lysosomes after a time-dependent transition in the endocytic pathway (Hurtado-Lorenzo et al., 2006). Immune complexes that contained the anti-myc monoclonal and Alexa Fluor 488-conjugated anti-mouse IgG antibodies co-localized significantly, but only in part, with BSA-Alexa Fluor 594 3 h after bradykinin treatment (Fig. 6, bottom; proportion of co-localized intracellular particles 1.4% in 75 control cells, 20.0% in 53 bradykinin-treated cell, $P<0.001$ by χ^2 test).

4. Discussion

An increasing number of conjugates uniting cargoes to agonists of various receptors are being reported in the literature. An example of this is given by the conjugation of substance P with fragments of synthetic antibody (Rizk et al., 2009), which supports the idea that a G-protein coupled receptor, in this case NK-1, can mediate transport of a cargo larger than its natural ligand. Furthermore, the cargo could escape the endocytic system and seemed to retain its activity. Another example is reported by Diagaradiane et al. (2008), where EGF was conjugated to Qdots nanocrystals, a strategy allowing higher performance imaging of EGF receptor-overexpressing tumors. Because of the severe loss of affinity for the B_2 receptor exhibited by carboxyfluorescein-ε–aminocaproyl-bradykinin due to the modification of the ligand structure (Gera et al., 2011), this is probably not the optimal path to increase the variety of cargoes that can be accommodated by the bradykinin B_2 receptor.

Therefore, for further biotechnological applications, we next turned our focus towards anti-receptor antibodies and the possibility of using antibodies conjugated with different types of cargoes, which would be internalized while bound to the receptor, itself stimulated by its ligand. After validating the endocytosis of a single anti-myc antibody bound to the receptor encoded by myc-B_2R (Figs. 1, 2; two different anti-myc clones used: clone 4A6 and clone 9E10), we assessed the internalization of a complex composed of the receptor, the anti-receptor antibody (anti-myc clone 4A6), and a secondary antibody coupled either to a fluorophore (the goat anti-mouse antibodies used in these experiments were coupled to Alexa fluor-594 or -488) or to the much brighter quantum dot fluorescent nanomaterials, following agonist treatment. This

approach confirmed the hypothesis that suggested that a G protein coupled receptor can transport molecules much larger than its ligand in the cell when internalized. Within the limitations of the trafficking study approach, that usually involved the overexpression of fluorescent subcellular markers with occasional unexpected effects, the mechanisms of endocytosis recruited by the receptor-anti-receptor antibody-secondary antibody appear to be identical to the ones normally mobilized, as illustrated by the rapid co-localization of β-arrestin$_2$ to the endosomes containing the immune complexes (Fig. 7, schematic representation of trafficking). The latter are also positive for early endosome autoantigen-1, an effector of the small G protein Rab5 (Grosshans et al., 2006). The size of an immune complex assembled at the cell surface is theoretically quite large if the ratio is 1 receptor: 1 anti-receptor antibody: 1 secondary antibody, which amounts to a size of approximately 370 kDa. However, there is probably the formation of multivalent complexes where one antibody can couple two receptors and so forth. The immune complexes that include Qdots 705 are even larger, in the order of 1.5 megadaltons for the nanoparticle itself (Lin et al., 2008), not counting its polymer and F(ab')$_2$ antibodies coatings (average of 3 antibody molecules per particle according to the manufacturer). Nevertheless, it seems that the trafficking of the examined immune complexes is dissociable from that of bradykinin-stimulated myc-tagged B_2 receptors, as the complexes persist in intracellular structures that are partly labelled with GFP-Rab7 after 3 h (Fig. 6), a time point where bradykinin is disposed of in the serum-containing culture medium ($t_{1/2}$ < 10 min) and the B_2 receptor recycled to the cell surface (Bachvarov et al., 2001). This is analogous to the retention of Qdots coated with transferrin in cells, while the transferrin receptors are rapidly recycled to the cell surface (Tekle et al., 2008).

Fig. 3 shows the lack of agonist effect of the anti-myc antibody clone 4A6 on myc-tagged B_2 receptors, as there is no elevation of calcium transients, a hallmark of receptor activation. Abd Alla et al. (1996) have mapped the sites of peptide agonist and antagonist binding in the bradykinin B_2 receptor with the aid of antibodies directed against various regions of the human B_2 receptor extracellular domains, and found that the N-terminal binding site of the antibody is not situated at the agonist or antagonist binding site. Docking models of LF 16-0687 to the human B_2 receptor do not involve interaction with the receptor N-terminal region (Marie et al., 2001). Accordingly, the anti-myc antibody does not activate the receptor and does not either impede the binding of the agonist (allowing internalization of the receptor following agonist treatment or failing to antagonize BK-induced calcium transient). Furthermore, it does not impair binding of the nonpeptide antagonist LF 16-0687, as this compound still prevents internalization of the immune complex when cells are co-incubated with bradykinin.

A certain level of agonist-independent aggregation of anti-myc antibodies at the cell surface and of agonist-independent background endocytosis has been evidenced using all detection systems (Figs. 1, 4). Whether this background can be reduced, e.g., by using monovalent anti-receptor antibodies, remains to be seen; anti-receptor antibody-based cargoes could lead to a multitude of applications. Here we have mainly exploited the possibility to enhance imaging of our receptor of interest, the bradykinin B_2 receptor, conjugated to an antigenic tag accessible to an antibody present in the extracellular space. This limitation is imposed by the scarcity of antibodies that recognize extracellular epitopes present in intact receptors, and raising or selecting such antibodies for this and other G protein coupled receptor remains a valid goal to expand this approach. We have also aimed to test the ability of a receptor to internalize into intact cells in response to its agonist, when included in a larger complex, constituted of antibodies. The addition

of functional moieties to the antibodies bound to the internalizing G protein coupled receptor may lead to the generation of new types of signalling events by the receptor depending on the presence of the agonist.

Aside from small ligand-conjugated cargoes, very large antibody-based cargoes can be transported by agonist-stimulated B_2 receptors into intact cells. These cargoes require a receptor competent for interaction with β-arrestins and they enter a Rab7-positive degradation pathway within 3 h.

Acknowledgements

This work was supported by the grant MOP-93773 to F.M. from the Canadian Institutes for Health Research. M.-T.B. is the recipient of a Studentship Award from the Fonds de la recherche en Santé du Québec. We thank Drs. Marc Pouliot, Normand Marceau and Paul Naccache (CHUQ) for facilitating the access to microscopic and fluorometric equipments.

References

Abd Alla, S., Quitterer, U., Grigoriev, S., Maidhof, A., Haasemann, M., Jarnagin, K., Müller-Esterl, W., 1996. Extracellular domains of the bradykinin B2 receptor involved in ligand binding and agonist sensing defined by anti-peptide antibodies. J. Biol. Chem. 271, 1748-1755.

Bachvarov, D.R., Houle, S., Bachvarova, M., Bouthillier, J., Adam, A., Marceau, F., 2001. Bradykinin B_2 receptor endocytosis, recycling, and down-regulation assessed using green fluorescent protein conjugates. J. Pharmacol. Exp. Ther. 297, 19-26.

Bawolak, M.T., Fortin, S., Bouthillier, J., Adam, A., Gera, L., C.-Gaudreault, R., Marceau, F., 2009, Effects of inactivation-resistant agonists on the signalling, desensitization and down-regulation of bradykinin B_2 receptors. Br. J. Pharmacol. 158, 1375-1386.

Bawolak, M.T., Gera, L., Bouthillier, J., Stewart, J.M., Adam, A., Marceau, F. 2008. A fluorescent version of the bradykinin B_2 receptor antagonist B-9430: pharmacological characterization and use in live cell imaging. Peptides 29, 1626-1630.

Bawolak, M.T., Gera, L., Morissette, G., Stewart, J.M., Marceau, F., 2007. B-9972 (D-Arg-[Hyp^3,Igl^5,Oic^7,Igl^8]-bradykinin) is an inactivation-resistant agonist of the bradykinin B_2 receptor derived from the peptide antagonist B-9430 (D-Arg-[Hyp^3,Igl^5,D-Igl^7,Oic^8]-bradykinin): pharmacologic profile and effective induction of receptor degradation. J. Pharmacol. Exp. Ther. 323, 534-546.

Bernier, V., Lagacé, M., Lonergan, M., Arthus, M.F., Bichet, D.G., Bouvier, M., 2004. Functional rescue of the constitutively internalized V2 vasopressin receptor mutant R137H by the pharmacological chaperone action of SR49059. Mol. Endocrinol. 18, 2074-2084.

Diagaradjane, P., Orenstein-Cardona, J.M., Colón-Casasnovas, N.E., Deorukhkar, A., Shentu, S., Kuno, N., Schwartz, D.L., Gelovani, J.G., Krishnan, S., 2008. Imaging epidermal growth factor receptor expression in vivo: pharmacokinetic and biodistribution characterization of a bioconjugated quantum dot nanoprobe. Clin. Cancer Res. 14, 731-741.

Gera, L., Bawolak, M.-T., Roy, C., Lodge, R., Marceau, F, 2011. Design of fluorescent bradykinin analogs: application to imaging of B_2 receptor-mediated agonist endocytosis and trafficking and of angiotensin converting enzyme. J. Pharmacol. Exp. Ther. 337, 33-41.

Grosshans, B.L., Ortiz, D., Novick, P., 2006. Rabs and their effectors: achieving specificity in membrane traffic. Proc. Natl. Acad. Sci. U.S.A. 103, 11821-11827.

Hurtado-Lorenzo, A., Skinner, M., El Annan, J., Futai, M., Sun-Wada, G.H., Bourgoin, S., Casanova, J., Wildeman, A., Bechoua, S., Ausiello, D.A., Brown, D., Marshansky, V., 2006. V-ATPase interacts with ARNO and Arf6 in early endosomes and regulates the protein degradative pathway. Nat. Cell Biol. 8, 124-136.

Kabeya, Y., Mizushima, N., Ueno, T., Yamamoto, A., Kirisako, T., Noda, T., Kominami, E., Ohsumi, Y., Yoshimori, T., 2000. LC3, a mammalian homologue of yeast Apg8p, is localized in autophagosome membranes after processing. EMBO J. 19, 5720-5728.

Kutateladze, T.G., Ogburn, K.D., Watson, W.T., de Beer, T., Emr, S.D., Burd, C.G., Overduin, M., 1999. Phosphatidylinositol 3-phosphate recognition by the FYVE domain. Mol. Cell 3, 805-811

Leeb-Lundberg, L.M.F., Marceau, F., Müller-Esterl, W., Pettibone, D.J., Zuraw, B.L., 2005. International Union of Pharmacology. XLV. Classification of the kinin receptor family: from molecular mechanisms to pathophysiological consequences. Pharmacol. Rev. 57, 27-77.

Lin, P., Chen, J.W., Chang, L.W., Wu, J.P., Redding, L., Chang, H., Yeh, T.K., Yang, C.S., Tsai, M.H., Wang, H.J., Kuo, Y.C., Yang, R.S.H., 2008. Computational and ultrastructural toxicology of a nanoparticle, quantum dot 705, in mice. Environ. Sci. Technol. 42, 6264-6270.

Marceau, F., Bawolak, M.T., Bouthillier, J., Morissette, G., 2009. Vacuolar ATPase-mediated cellular concentration and retention of quinacrine: a model for the distribution of lipophilic cationic drugs to autophagic vacuoles. Drug Metab. Dispos. 37, 2271-2274.

Marie, J., Richard, E., Pruneau, D., Paquet, J.L., Siatka, C., Larguier, R., Poncé, C., Vassault, P., Groblewski, T., Maigret, B., Bonnafous, J.C., 2001. Control of conformational equilibria in the human B_2 bradykinin receptor. Modeling of nonpeptidic ligand action and comparison to the rhodopsin structure. J. Biol. Chem, 276, 41100-41111.

Munoz, C.M., Leeb-Lundberg, L.M.F., 1992. Receptor-mediated internalization of bradykinin.DDT1 MF-2 smooth muscle cells process internalized bradykinin via multiple degradation pathways. J. Biol. Chem. 267, 303-309.

Rizk, S.S., Luchniak, A., Uysal, S., Brawley, C.M., Rock, R.S., Kossiakoff, A.A., 2009. An engineered substance P variant for receptor-mediated delivery of synthetic antibodies into tumor cells. Proc. Natl. Acad. Sci. U.S.A. 106, 11011-11015.

Tekle. C., van Deurs, B., Sandvig, K., Iversen, T.G., 2008. Cellular trafficking of quantum dot-ligand bioconjugates and their induction of changes in normal routing of unconjugated ligands. Nano Lett, 8, 1858-1865.

Figure legends

Figure 1. A. Microscopic analysis of cortical and intracellular fluorescence in a microphotography of an intact HEK 293a cell. Epifluorescence, original magnification 1000×. See Materials and methods for description. B. and C. Endocytosis assays of a monoclonal antibody cargo mediated by receptors encoded by the myc-B_2R vector in live HEK 293 cells. Labelling with either monoclonal antibody 4A6 or 9E10 (1:1000 dilution for either; the latter antibody purchased from Covance) was performed at room temperature, the cells were washed and then incubated at 37°C in serum-free culture medium. Optionally, cells were further stimulated with the agonist bradykinin (BK; 10 nM) for the last 15 minutes of the incubation period. Thereafter, the cells were fixed, permeabilized and stained with the secondary Alexa Fluor 488-labeled antibody. Confocal microscopy (BioRad 1024 apparatus; sides of square fields = 60 µm).

Fig. 2. Proportion of cortical (membrane-associated) fluorescence in HEK 293 cells transiently transfected with the myc-B_2R vector and submitted to the receptor-antibody internalization assay (sample confocal photographic record in Fig. 1). The Mann-Whitney test indicated a significant loss of membrane-associated fluorescence, relative to the intracellular fluorescence, in cells stimulated with bradykinin (BK).

Fig. 3. Calcium mobilization in HEK 293a cells transiently transfected with the myc-B_2R vector: acute effect of ligands (BK, bradykinin, or the monoclonal antibody 4A6). The antibody (1:1000) or its saline vehicle were conventionally applied at the time -50 sec, and the agonist (10 nM) or

its saline vehicle at 0 sec (arrows). Conventionally, the differences in the intracellular calcium concentrations are calculated relative to time zero. Values are mean ± S.E.M. of 2 determinations.

Fig. 4. Endocytosis of anti-myc 4A6 monoclonal complexed to Qdots coated with anti-mouse IgG antibodies by intact HEK 293a cells expressing myc-tagged B_2 receptors or its truncated form and pharmacologically treated as indicated at 37°C (BK, bradykinin). Each field is shown as a pair of images: epifluorescence in intact cells (left); phase contrast view (right). Representative results of 4 separate days of experiments. Original magnification 1000 × (nt: nontransfected cells).

Fig. 5. Proportion of cortical (membrane-associated) fluorescence in HEK 293a cells transiently transfected with the myc-B_2R or myc-B_2R_{trunc} vectors and submitted to the Qdot-antibody internalization assay (sample photographic record in fig. 4; BK, bradykinin). The number of evaluated cells is indicated above each histogram. The Kruskal-Wallis test indicated that the values were heterogenous ($P<0.001$). The effect of drug treatment relative to the appropriate control was evaluated using Dunn's multiple comparison test. * $P<0.001$.

Fig. 6. Top 4 rows: Endocytosis of anti-myc 4A6 monoclonal antibodies complexed to Qdots coated with anti-mouse IgG antibodies (red fluorescence) by intact HEK 293a cells transiently transfected with the myc-B_2R vector and, optionally, with an additional vector coding for another transgene (as indicated). Cells were further pharmacologically stimulated at 37°C (BK, bradykinin). Bottom row: Endocytosis of anti-myc 4A6 monoclonal complexed to anti-mouse immunoglobulins conjugated to a green fluorophore by intact HEK 293a cells co-treated with BSA-Alexa fluor 594. Epifuorescence, original magnification 1000×. In the co-localization

experiments, the white arrowheads point to examples of the salient findings. See Results for statistical analysis of co-localization experiments.

Fig. 7. Schematic representation of the mechanisms of bradykinin B_2 receptor-mediated uptake of cargoes in intact cells. The serpentine line represents the myc-tagged B_2 receptor, the small rectangle, the agonist bradykinin (BK), and the antibody coupled to a circle, the anti-myc antibody coupled to cargo.

A. Defining cortical and intracellular zones

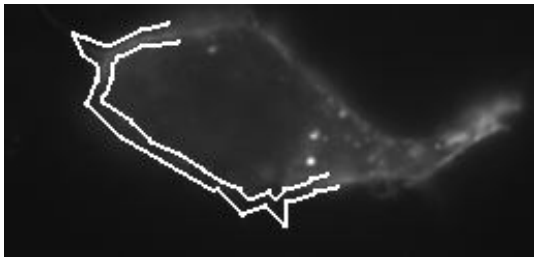

B. Anti-myc monoclonal 4A6 labelling on live cells

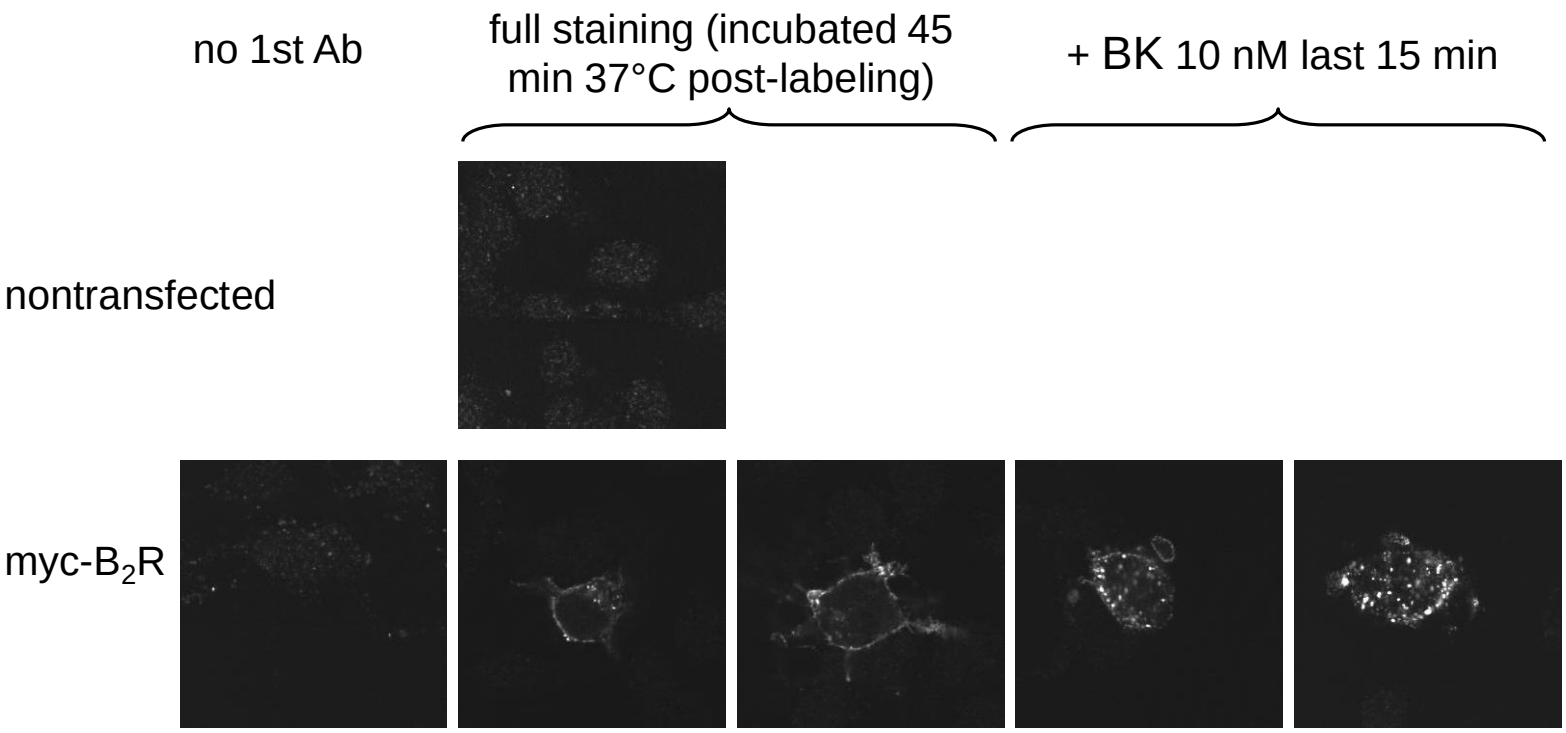

C. Anti-myc monoclonal 9E10 labelling on live cells

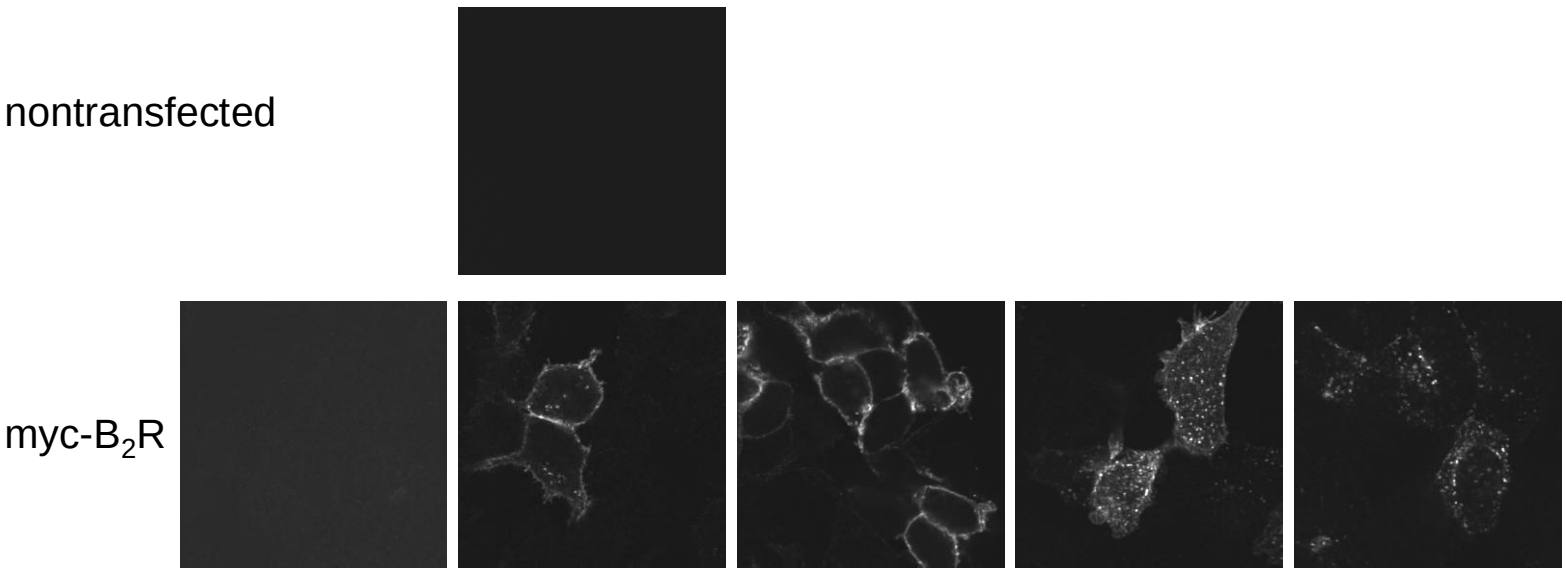

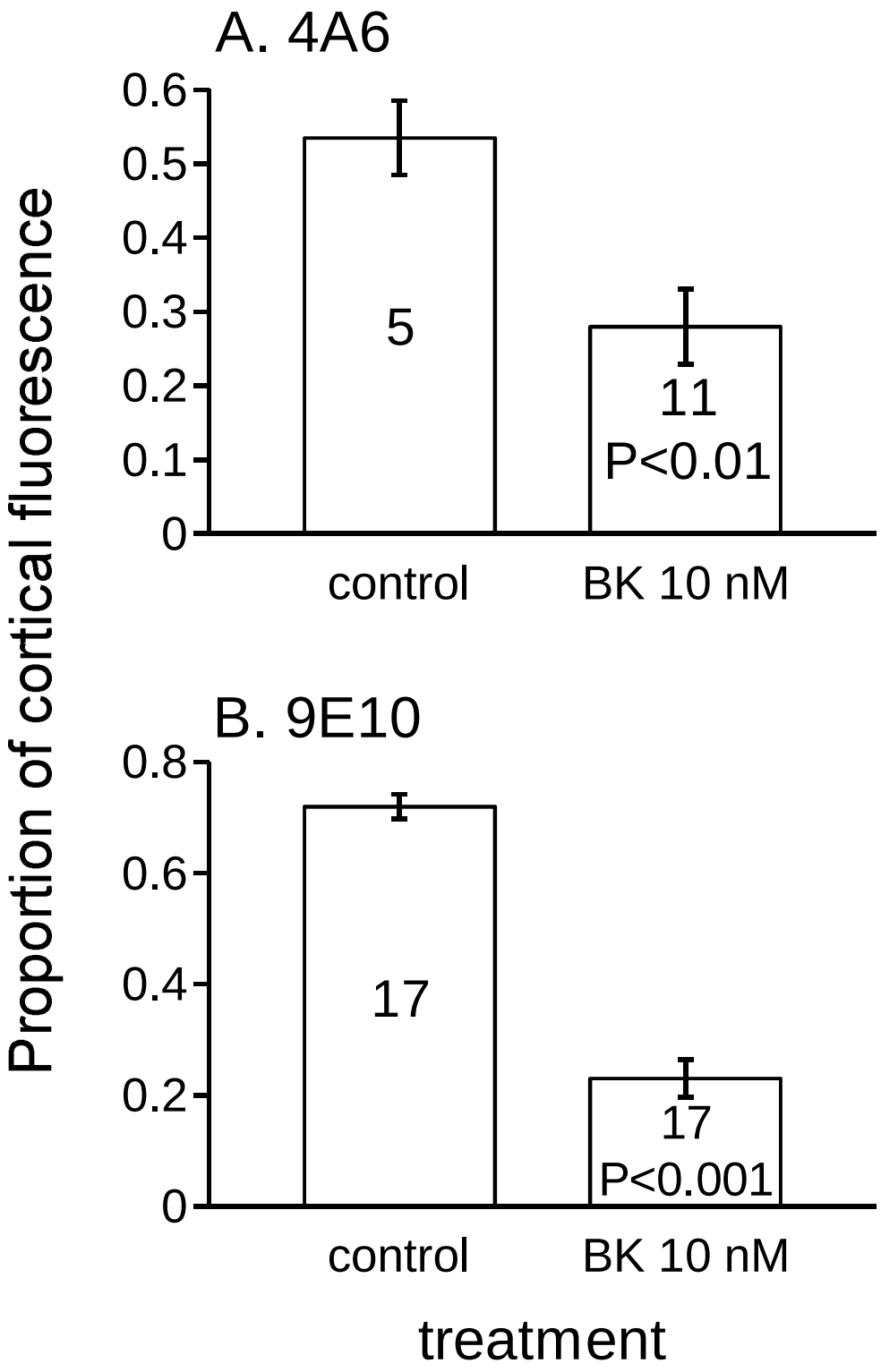
A. 4A6
0.6
0.5
0.4
0.3
0.2
0.1
0
5
11
P<0.01
control
BK 10 nM
B. 9E10
0.8
0.6
0.4
0.2
0
17
17
P<0.001
control
BK 10 nM
Proportion of cortical fluorescence
treatment

Figure 3

Fig. 3

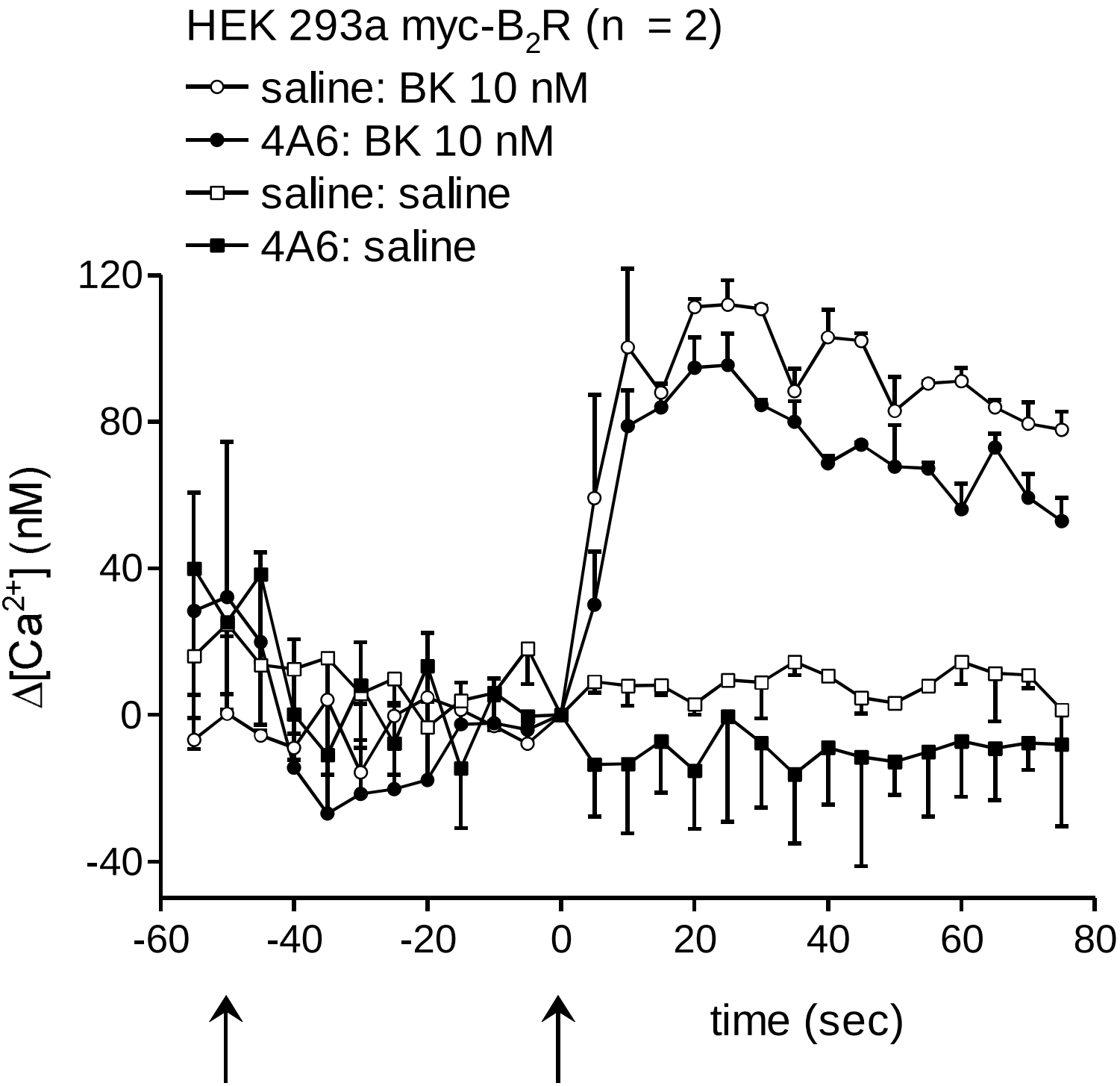

4A6 + Qdots 705

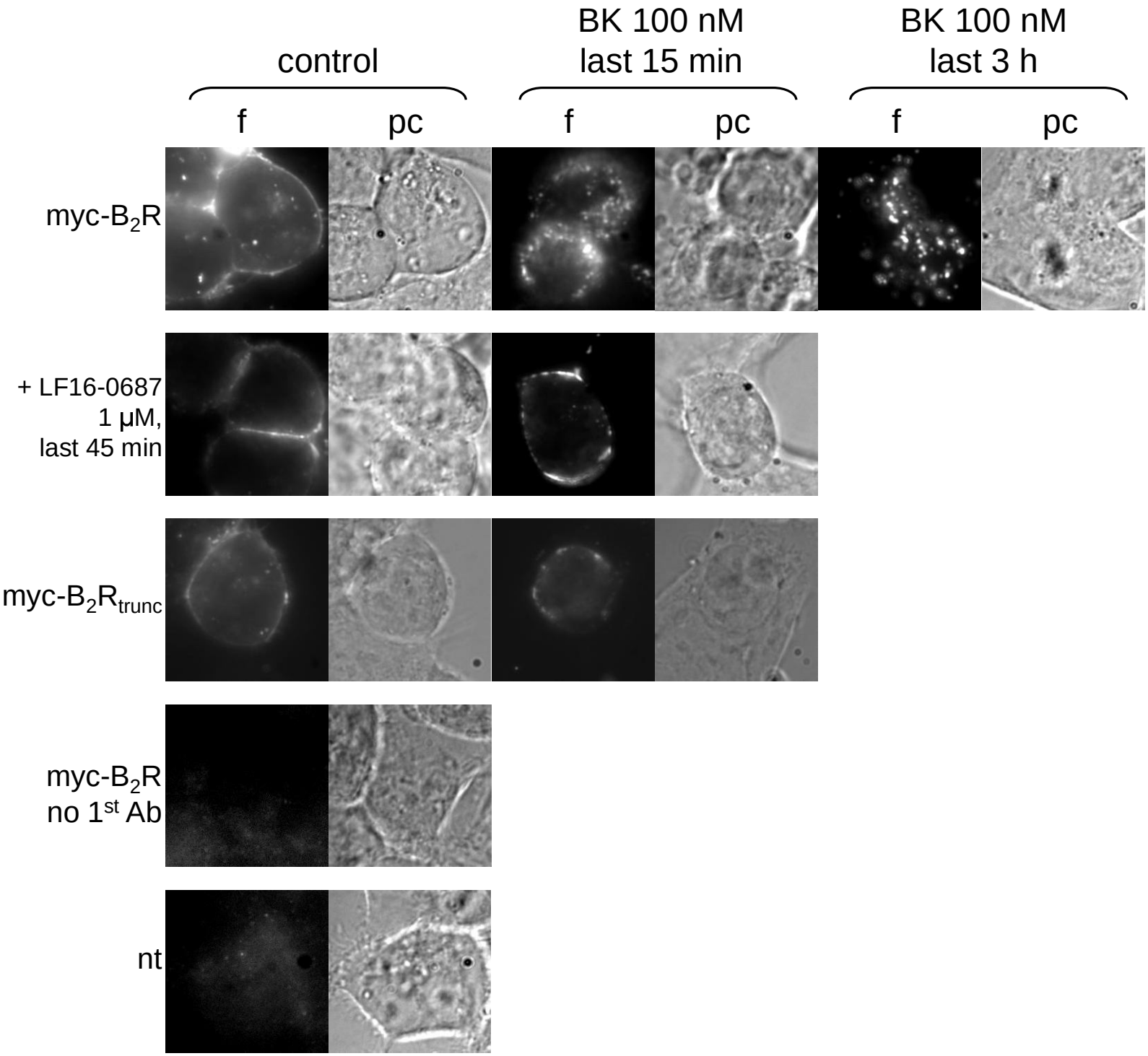

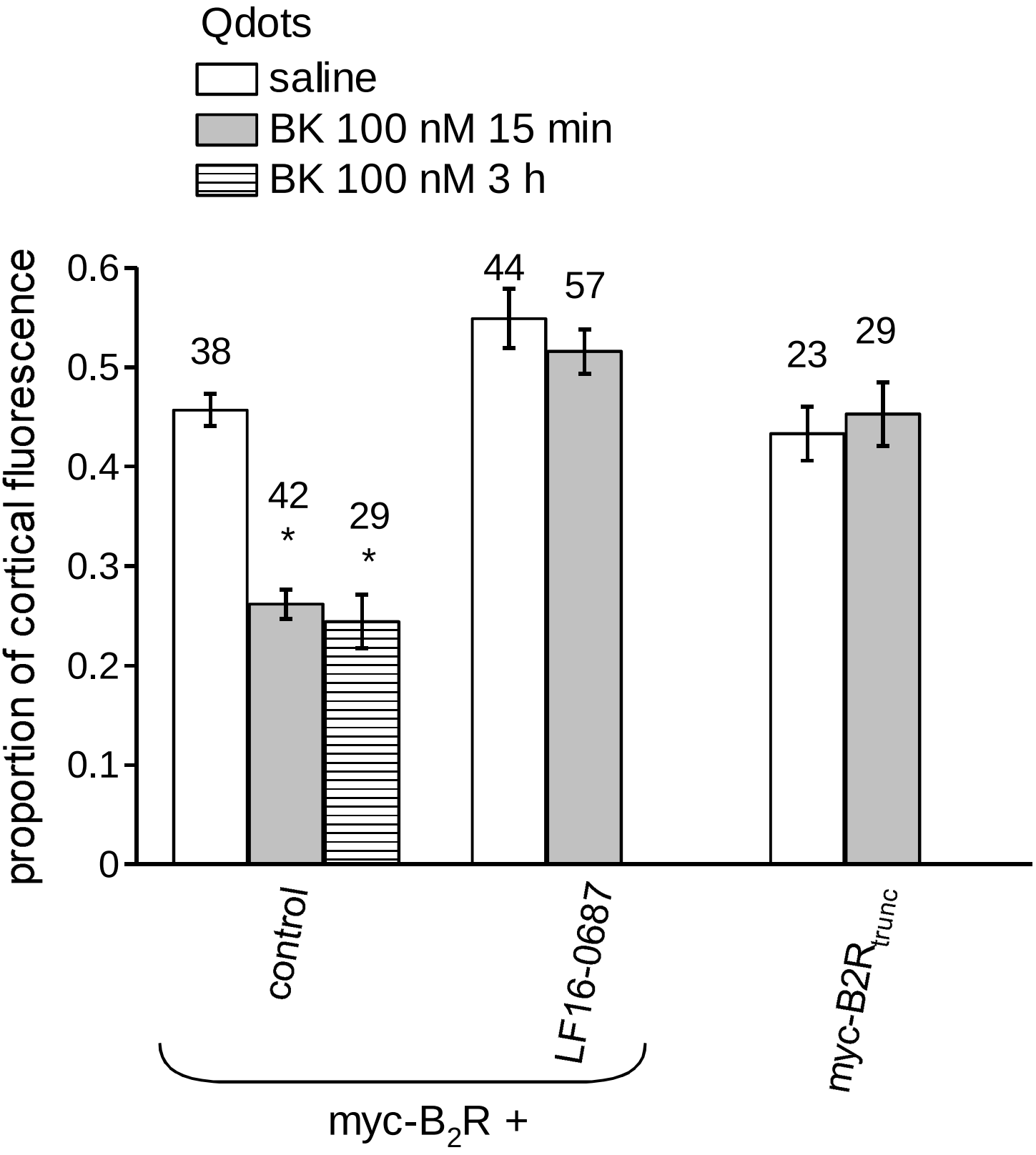
Qdots
saline
BK 100 nM 15 min
BK 100 nM 3 h
proportion of cortical fluorescence
0.6
0.5
0.4
0.3
0.2
0.1
0
38
42
*
29
*
44
57
23
29
control
LF16-0687
myc-B2R$_{trunc}$
myc-B$_2$R +

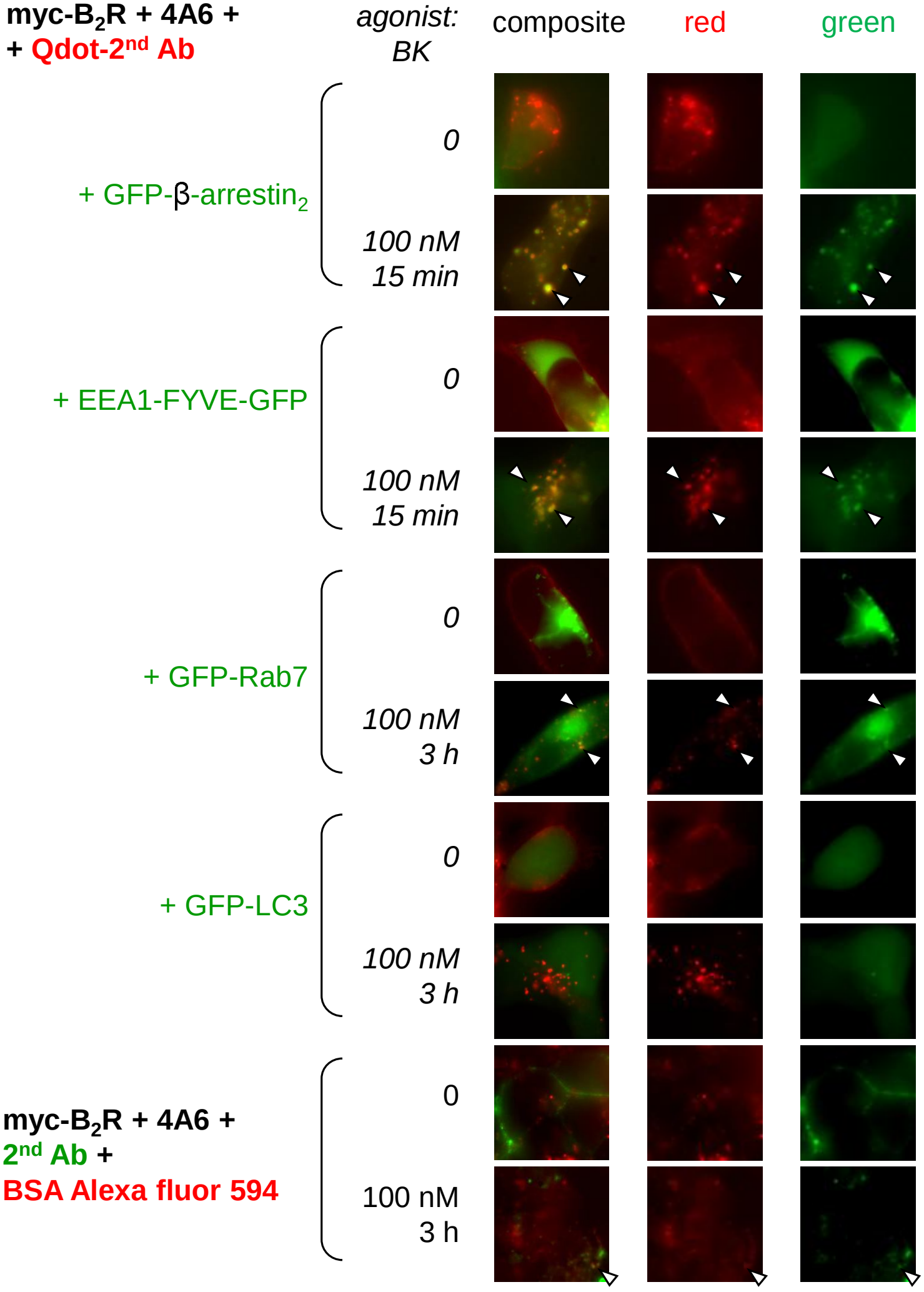
myc-B2R + 4A6 +
+ Qdot-2nd Ab
agonist:
BK
composite
red
green
+ GFP-β-arrestin2
0
100 nM
15 min
+ EEA1-FYVE-GFP
0
100 nM
15 min
+ GFP-Rab7
0
100 nM
3 h
+ GFP-LC3
0
100 nM
3 h
myc-B2R + 4A6 +
2nd Ab +
BSA Alexa fluor 594
0
100 nM
3 h

Figure 7
Fig. 7